Creeping Flows In and Around a Compound Multiphase Droplet

Prabir Daripa and D. Palaniappan
Department of Mathematics, Texas A&M University
College Station, TX 77843, e-mail: prabir.daripa@math.tamu.edu

Abstract

Exact analytical solutions for steady-state axisymmetric creeping flow of a viscous incompressible fluid in the presence of a compound multiphase droplet are derived. The two spherical surfaces constituting a vapor-liquid compound droplet are assumed to overlap with a contact angle $\pi/2$. It is further assumed that the surface tension forces are sufficiently large so that the interfaces have uniform curvature. The singularity solutions for the flow induced by a stokeslet in the presence of a compound droplet are obtained by the method of reflections. The flow patterns are discussed in the case of a flow induced by a pair of opposite stokeslets. Toroidal eddy patterns are observerd in the continous phase for some fixed value of the viscosity ratio. The eddy changes its size and shape if the locations of the initial stokeslets are altered. These observations may be useful in the study of hydrodynamic interactions of droplets with other objects in a viscous fluid. We also provide a brief discussion of our results in connection with the computation of mobility functions. The exact results presented here can be useful in validating numerical algorithms and codes on multiphase flow and fluid-droplet interactions.

1 Introduction

In recent years, there has been a general surge of interest in understanding the behavior of compound multiphase drops as a result of their occurrence in a variety of engineering systems. These drops occur in processes such as melting of ice particles in the atmosphere, liquid membrane technology as well as in other industrial operations. Gas-liquid compound drops are also found as transient configurations during rapid evaporations of drops near the super heat limit [1] and disruptive combustion of free droplets of multi-component fuels [2]. The studies concerning the lipid bilayer [3] and polymer grafted [4] membranes in concentrated solutions also reveal the existence of compound drops. The experimental evidences recorded in those studies initiated the relevant theoretical investigations in the last few decades.

Some perspectives on the theoretical fluid mechanics of multiphase droplets are discussed for instance in Avedisian and Andres [5], Johnson and Sadhal [6], Sadhal et. al. [7] among many others. The compound drop is usually modeled as two overlapping spherical surfaces with a contact angle. This model has been used in the electric field-induced cell-to-cell fusion process to predict the fusion of biological cells [8]. In hydrodynamics, similar models have been employed to analyze the flow fields in and around a compound droplet [9, 10, 11]. In [9], the translation of a vapor-liquid compound drop was solved by the use of toroidal frame. The expressions for the flow fields and hydrodynamic force were obtained in terms of a rather complicated conical functions. For the overlapping spheres with a contact angle $\pi/2$, simple singularity solutions for the Stokes flow past an encapsulated droplet (compound drop) were presented later in [10]. This simple approach has been further exploited more recently in [11] to derive solutions for a compound drop suspended in complicated flow fields. The analyses provided in [10, 11] form the basis for the present study.

We discuss here some flow patterns in connection with droplet-fluid interactions in complex flow situations. In particular, we provide singularity solutions for axisymmetric flow induced by a stokeslet in the presence of a compound droplet which describe the flow fields in the continuous and dispersed phase fluid regions, respectively. The flow patterns displayed here explains the flow behavior in and around a compound droplet suspended in stokeslet induced flows. The plots of drag force acting on the droplet illustrate several interesting features. The calculations of the present study can

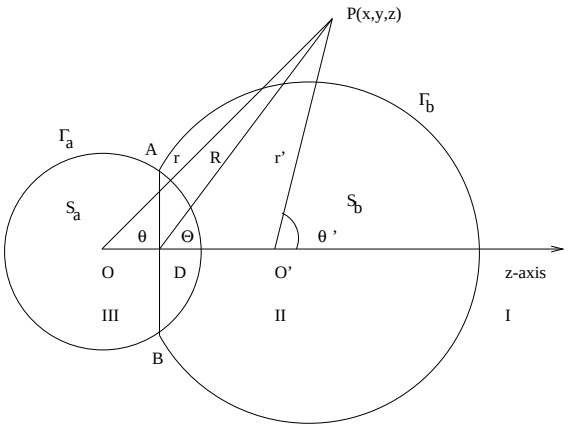

Figure 1: Schematic of a vapor-liquid compound droplet Γ

provide the basis for computing mobility functions. It is worth mentioning here that one of the primary motivations behind this work has been to provide exact solutions to somewhat complicated, yet analytically tractable, problems that can be used to validate numerical algorithms and codes on multiphase flow and fluid-droplet interactions.

2 Geometry of the compound droplet

The two-sphere geometry of the compound droplet is depicted in Fig. 1. This geometry consists of two unequal overlapping spheres S_a and S_b of radii a and b with centers O and O' respectively. We assume that these spheres intersect orthogonally. The boundary of the droplet is denoted by $\Gamma = \Gamma_a \cup \Gamma_b$, where Γ_a is part of the boundary where $r = a$ and Γ_b is part of the boundary where $r = b$ (see Fig. 1). Since the spheres overlap at a contact angle $\pi/2$, the two centers share a common inverse point D. In the right-angled triangle OAO', $c^2 = a^2 + b^2$, where $OO' = c$. In the meridian plane, the line AB intersects OO' at D. Hence, $OD = a^2/c$ and $DO' = b^2/c$. Let $(r, \theta, \phi), (r', \theta', \phi)$ and (R, Θ, ϕ) be the spherical polar coordinates of any point outside the assembly Γ with O, O' and D as origins respectively. The geometrical relations that follow from Fig. 1 are given in [11].

Part of the sphere S_b contains a liquid with viscosity different from the viscosity of the liquid around the droplet, and part of the sphere S_a contains

vapor. It should be remarked that the interface separating the vapor and the dispersed phase liquid joins points A and B, and is not the the line AB shown in the Fig. 1. This interface between the phases is assumed to have a uniform curvature different from that of the spheres S_a and S_b. We designate the fluid region exterior to Γ as I and the spherical regions S_b and S_a as II and III respectively. The surface tension forces are assumed to be large enough to keep the interfaces in a spherical shape. The vapor-liquid configuration exists at rest with contact angle approximately 90^o if $\gamma_{I,II} \approx \gamma_{II,III} >> \gamma_{I,III}$ which is in agreement with the Laplace law on all interfaces. Here the $\gamma_{a,b}$ denotes the surface tension at the interface separating regions a and b.

3 Formulation of the Problem

We consider a stationary compound drop submerged in an arbitrary axisymmetric flow of a viscous fluid. The Reynolds number of the flow fields is assumed to be small so that all inertial effects are negligible. In this case, the governing equations for fluid flow are the linearized steady Navier-Stokes equations, also called creeping flow equations or Stokes equations,

$$\mu^{(i)}\nabla^2\mathbf{q}^{(\mathbf{i})} = \nabla p^{(i)}, \quad \nabla\cdot\mathbf{q}^{(\mathbf{i})} = 0, \tag{1}$$

where $i = 1, 2$ refers to continuous and dispersed phase liquids respectively, $\mathbf{q}^{(\mathbf{i})}, p^{(i)}$ and $\mu^{(i)}$ are the velocities, pressures and viscosities in the respective phases. The boundary and interface conditions are as follows: (i) velocity and pressure far from the droplet are that of the underlying flow; (ii) zero normal velocity on Γ; (iii) continuity of tangential velocity and shear stress at the liquid-liquid interface Γ_b; and (iv) zero shear-stress at the vapor-liquid interface Γ_a. The governing Stokes equations subject to the above far-field and interface conditions constitute a well-posed problem whose solution provides the velocities and pressures prevailing in the presence of the compound droplet.

As the flow is axially symmetric about the $z-$axis, it is convenient to use the Stokes stream function formulation which requires the solution of the fourth-order scalar equation

$$L^2_{-1}\psi = 0, \tag{2}$$

where L_{-1} is the axisymmetric Stokes operator given by

$$L_{-1} = \frac{\partial^2}{\partial r^2} + \frac{1-\eta^2}{r^2}\frac{\partial^2}{\partial \eta^2}, \tag{3}$$

for the coordinates (r, θ) with $\eta = \cos\theta$. Now the velocity components in terms of the stream function are given by

$$q_r^{(i)} = \frac{1}{r^2 \sin\theta}\frac{\partial \psi^{(i)}}{\partial \theta}, \quad q_\theta^{(i)} = -\frac{1}{r \sin\theta}\frac{\partial \psi^{(i)}}{\partial r}, \tag{4}$$

and the pressure is obtained from

$$\frac{\partial p^{(i)}}{\partial r} = -\frac{\mu^{(i)}}{r^2 \sin\theta}\frac{\partial}{\partial \theta}(L_{-1}\psi^{(i)}), \quad \frac{\partial p^{(i)}}{\partial \theta} = \frac{\mu^{(i)}}{\sin\theta}\frac{\partial}{\partial r}(L_{-1}\psi^{(i)}). \tag{5}$$

The boundary and the interface conditions stated at the beginning of this section can also be expressed in terms of the stream function (see [11] for details).

4 Results

The solutions for the above problem for various axisymmetric underlying flows can be obtained by the method of successive reflections. Since the two spheres intersect at a contact angle $\pi/2$, it is easy to see that the solutions are arrived at the third reflection. The solutions are conveniently represented in cylindrical coordinates if we define $(\rho, \phi, z), (\rho', \phi, z')$ and (Π, ϕ, Z) as the cylindrical polar coordinates with respect to O, O' and D as origins, respectively (see Fig. 1).

We now consider the underlying flow to be the flow induced by a stokeslet of strength $\frac{D_3}{8\pi\mu^{(1)}}$, located at a point $(0, 0, c+d)$, say E_1, outside Γ. The free-space stream function due to this stokeslet is $\psi_0(\rho, z) = \frac{D_3}{8\pi\mu^{(1)}}\frac{\rho_1^2}{r_1}$, where (ρ_1, z_1) are the cylindrical coordinates with E_1 as origin. The flow fields in the presence of a compound droplet with a stokeslet outside it can be obtained by taking continous reflections as explained in [10, 11]. For the sake of brevity, we omit the details and give here the solutions in the respective

phases. For the continous phase, the solution is

$$\begin{aligned}\psi^{(1)}(\rho,z) &= \frac{D_3}{8\pi\mu^{(1)}}\frac{\rho_1^2}{r_1} - \frac{D_3}{8\pi\mu^{(1)}}\frac{a}{c+d}\frac{\rho_2^2}{r_2} + \frac{D_3}{8\pi\mu^{(1)}}\Lambda\Bigg[-\frac{b}{2d}\left(3-\frac{b^2}{d^2}\right)\frac{\rho_3^2}{r_3} \\ &+ \frac{b^3\left(d^2-b^2\right)^2}{2d^5}\frac{\rho_3^2}{r_3^3} - \frac{b^3\left(d^2-b^2\right)}{(d^4}\frac{\rho_3^2 z_3}{r_3^3}\Bigg] - \frac{D_3}{8\pi\mu^{(1)}}(1-\Lambda)\frac{b}{d}\frac{\rho_3^2}{r_3} \\ &+ \frac{D_3}{8\pi\mu^{(1)}}\Lambda\Bigg\{\left[\frac{ab}{2(b^2+cd)}\left(3-\frac{b^2(c+d)^2}{(b^2+cd)^2}\right)\right]\frac{\rho_4^2}{r_4} \\ &- \frac{a^3b^3(d^2-b^2)(c+d)}{(b^2+cd)^4}\frac{\rho_4^2 z_4}{r_4^3} - \frac{a^5b^3(d^2-b^2)^2}{2(b^2+cd)^5}\frac{\rho_4^2}{r_4^3}\Bigg\} \\ &+ \frac{D_3}{8\pi\mu^{(1)}}(1-\Lambda)\frac{ab}{b^2+cd}\frac{\rho_4^2}{r_4}, \end{aligned} \tag{6}$$

and for the dispersed phase, the solution becomes

$$\begin{aligned}\psi^{(2)}(\rho,z) &= (1-\Lambda)\frac{(r'^2-b^2)}{2b^2}\frac{D_3}{8\pi\mu^{(1)}}\Bigg[-3+2r'\frac{\partial}{\partial r'} \\ &- \frac{(r'^2-b^2)}{2}L_{-1}\Bigg](\frac{\rho_1^2}{r_1} - \frac{a}{c+d}\frac{\rho_2^2}{r_2}), \end{aligned} \tag{7}$$

where $(\rho_2,z_2),(\rho_4,z_4),(\rho_4,z_4)$ are the cylindrical polar coordinates of a point with E_2,E_3,E_4 as origins respectively, and $r_j = r^2 - 2OO_j r\cos\theta + OO_j^2, j = 1,2,3,4$. Here $OO_1 = c+d, OO_2 = \frac{a^2}{c+d}, OO_3 = \frac{b^2+cd}{d}$ and $OO_4 = \frac{a^2 d}{b^2+cd}$ respectively. Note that E_2 and E_3 lie inside the spheres S_a and S_b respectively, but outside the overlap region and the point E_4 lies inside the overlap region. The image singularities are now located at these points (i.e., at E_2,E_3 and E_4). It is clear that the locations of the image points are indeed dictated by the location of the initial stokeslet. Now the image system in the continuous phase consists of stokeslets at E_2,E_3 and E_4, Stokes-doublets at E_3 and E_4 and Degenerate Stokes-quadrupoles at E_3 and E_4. The strengths of the image singularities depend on radii, the location of the initial stokeslet and the viscosity ratio. It is interesting to note that the image system for a stokeslet near a viscous drop also has the same type of singularities (with different strengths) as the compound drop. But the location of the image singularities in the former is at a single point. The solutions for a pair of stokeslets in the presence of a compound droplet may also be derived in a similar fashion.

Below we present the flow patterns for the case when the droplet is placed between two stokeslets of opposite strengths. We use the terminology "two

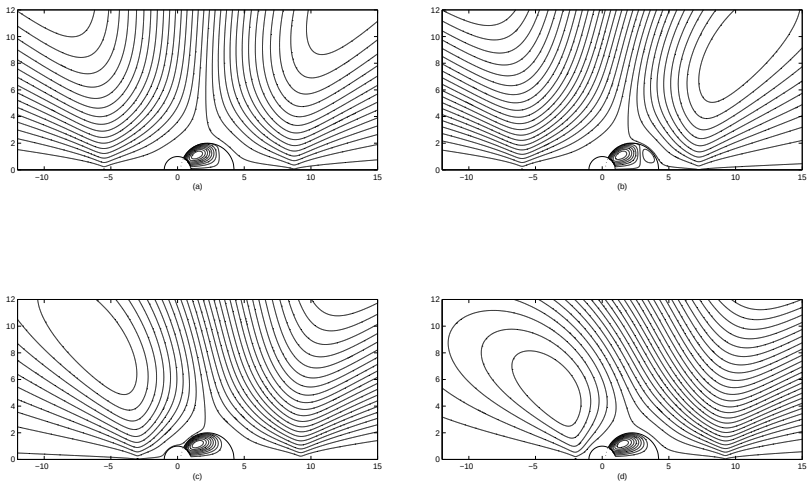

Figure 2: Flow patterns for a pair of opposite stokeslets with $a = 1$, $b = 2$, $\Lambda = 0.6$. (a) $d_b = b + 5, d_a = a + 5$, (b) $d_b = b + 3$, $d_a = a + 5$; (c) $d = b + 5$, $d_a = a + 2$; (d) $d = b + 5$, $d_a = a + 1$. Here d_b, d_a denote the locations of the stokeslets from the liquid and vapor spherical surfaces, respectively.

opposite stokeslets" to refer to two stokeslets: one with the positive strength, and the other with equal but negative strength. We choose the one which is on the vapor side to have positive strength and the other on the liquid side to have an equal but negative strength. Fig. 2(a)-(d) shows the flow patterns for the case of two opposite stokeslets for various locations. If the two stokeslets are far from the droplet, the interaction of the stokeslets is not stronger in the neighborhood of the droplet (see Fig. 2(a)). When they are moved closer, a single toroidal eddy structure appears in front of the liquid sphere. This eddy moves further close to the droplet as the stokeslets are moved nearer to the compound drop. We notice that the size and shape of these closed streamlines also change due to the stokeslets moving closer to the droplet. Since we have determined the solutions in singularity form, it is a straightforward task to derive formula for the drag force acting on the compound droplet. The strengths of the image stokeslets determine the drag and for the stokeslet induced flow the drag force (obtained from (6))

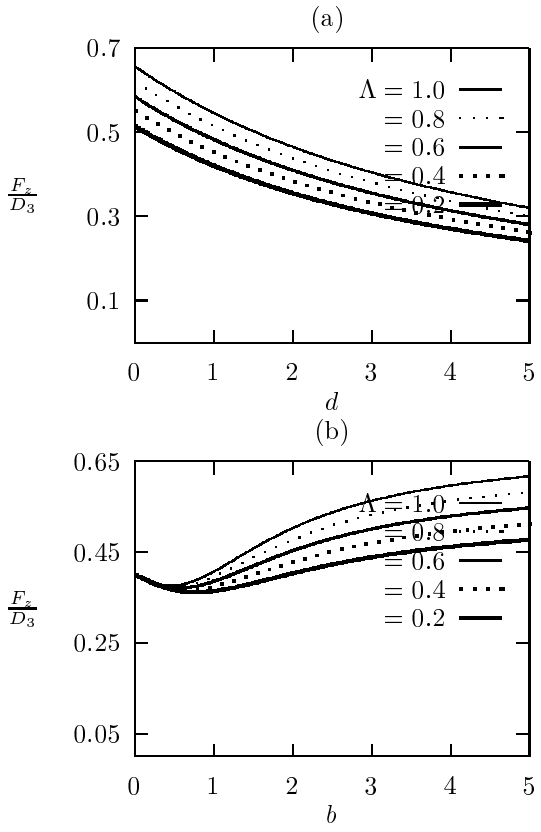

Figure 3: Drag force in a (single) stokeslet flow. (a) Variation with the stokeslet location d for a fixed $a = 1, b = 2$; (b) Variation with the liquid sphere radius b for a fixed $a = 2, d = b + 1$.

is

$$\begin{aligned} \mathbf{F} &= D_3\hat{e}_z\left\{\frac{a}{c+d} + \Lambda\left[\frac{b}{2d}\left(3 - \frac{b^2}{d^2}\right) - \frac{ab}{2(b^2+cd)}\left(3 - \frac{b^2(c+d)^2}{(b^2+cd)^2}\right)\right]\right. \\ &+ \left.(1-\Lambda)\left[\frac{b}{d} - \frac{ab}{b^2+cd}\right]\right\}. \end{aligned} \tag{8}$$

Here $\mathbf{F} = (F_x, F_y, F_z)$. It can be seen from (8) that the drag force on the compound drop in a stokeslet flow depends on the viscosity ratio, the radii and the location of initial stokeslet. We discuss briefly the variation of drag force with these parameters. In Fig. 3(a) we have plotted $\frac{F_z}{D_3}$ against the

location of the stokeslet d for different viscosity ratios with $a = 1$ and $b = 2$. The drag decreases monotonically with increasing values of d as expected. This means that the droplet experiences greater resistance in stokeslet flow if the stokeslet is closer to it. Fig. 3(b) shows variation of the drag force with radius 'b' when the stokeslet is at a distance $d = 1$. In this case, the drag force decreases until $b \approx 0.5$ and then starts increasing with increasing values of b. This, in turn, implies that the resistance is greater when the liquid volume is large compared to the vapor volume. It may be noticed that the drag force in general lies between the vapor-solid and vapor-vapor assembly limits. When $\Lambda = 1$, the expression (8) yields the force on a vapor-solid assembly while for $\Lambda = 0$, it reduces to the drag force on a vapor-vapor assembly (composite bubble).

4.1 Mobility functions

The image solutions for Stokes singularities may be employed in a method of reflections type of calculation for the interactions between a compound drop and an arbitrary small particle. The key idea is that over length scales associated with the compound drop, the disturbance fields produced by a small particle may be approximated by those produced by equivalent Stokes singularities (stokeslet, degenerate stokes-quadrupole etc.). In the reflections at the small sphere we can truncate the multipole expansion at the desired order in a_1/c_1, where a_1 is the radius of the smaller particle and c_1 is the distance between the location of the small particle and the center of the compound drop. For reflections at the large sphere, we retain the entire multipole solution, which of course is the image systems of the Stokes singularities. The mobility functions may then be computed in the same way as explained in [12]. The complete calculations of the mobility functions and the hydrodynamic interactions will be discussed elsewhere.

5 Acknowledgment

This research has been partially supported by the interdisciplinary research program of the Office of the Vice President for Research and Associate Provost for Graduate Studies under grant IRI-98.

References

[1] Shepherd, J. E., & Sturtevant, B. Rapid evaporation at the super heat limit. *J. Fluid Mech.,* **121**, pp. 379-402, 1982.

[2] Lasheras. J. C., Fernandez-pello, A. C., & Dryer, F. L. Experimental observations on the disruptive combustion of free droplets of multicomponent fuels. *Combust. Sci. Technol.,* **22**, pp. 195-209, 1980.

[3] Evans, E., & Needham, D. Attraction between lipid bilayer membranes in concentrated solutions of non-adsorbing polymers: Comparison of mean-field theory with measurements of adhesion energy. *Macromolecules* **21**, pp. 1822-1831, 1988.

[4] Evans, E., Klingenberg, D. J., Rawicz, W., & Szoka, F. Interactions between polymer-grafted membranes in concentrated solutions of free polymer. Pre-print, 1996.

[5] Avedisian, C. T., & Andres, R. P. Bubble nucleation in superheated liquid-liquid emulsions. J. Colloid Interface Sci. **64**, pp. 438-453, 1978.

[6] Johnson, R. E., & Sadhal, S. S. Fluid mechanics of compound multiphase drops and bubbles. *Ann. Rev. Fluid Mech.* **17**, pp. 289-320, 1985.

[7] Sadhal, S. S., Ayyaswamy, P. S., & Chung, J. N. Transport Phenomena with Drops and Bubbles. Springer-Verlag, New York, 1997.

[8] Zimmermann, U., & Vienken, J. Electric field-induced cell-to-cell fusion. *J. Memb. Biol.* **67**, pp. 165-182, 1982.

[9] Vuong, S. T., & Sadhal, S. S. Growth and translation of a liquid-vapor compound drop in second liquid. Part 1. Fluid Mechanics. *J. Fluid Mech.* **209**, pp. 617-637, 1987.

[10] Palaniappan, D. & Kim, S. Analytic solutions for Stokes flow past a partially encapsulated droplet. *Phys. Fluids* **A9(5)**, pp. 1218-1221, 1997.

[11] Palaniappan, D. & Prabir Daripa. Compound droplet in extensional and paraboloidal flows. *Phys. Fluids*, **12(10)**, pp. 2377-2385, 2000.

[12] Kim, S. & Karrila, S. J. Microhydrodynamics: Principles and Selected Applications. Boston: Butterwort-Heinemann, 1991.